Hydration of Apomyoglobin in Native, Molten Globule, and Unfolded States by Using Microwave Dielectric Spectroscopy

Takashi Kamei,* Motohisa Oobatake,[†] and Makoto Suzuki*

*Department of Metallurgy, Graduate School of Engineering, Tohoku University, Aoba-yama 02, Sendai, 980-8579, Japan; and [†]Faculty of Science and Technology, Meijo University, 1-501, Shiogamaguchi, Tenpaku-ku, Nagoya, 468-8502, Japan

ABSTRACT   The high resolution dielectric spectra of semidilute solutions of apomyoglobin in native (N, pH = 5), acid-induced molten globule (A, pH = 4), and unfolded (U_A, pH = 3) states have been measured in the range from 0.2 to 20 GHz. Based on a two-component mixture theory, we obtained the following hydration numbers per protein molecule: 590 ± 65 for N, 630 ± 73 for A, and 1110 ± 67 for U_A. There was no clear difference between N and A states in contrast to the 25% reduction of helix content and the 50% reduction of heat capacity change upon unfolding. This suggests that the association of hydrophobic moieties might follow the disruption of secondary structures from N to A states. The measured hydration number of U_A was close to that of the accessible water number (1340) of a protein molecule calculated for a fully extended structure, indicating that the structure of U_A is extended but somewhat more compact than that of a fully extended state.

INTRODUCTION

The protein folding process is one of the most intriguing issues in biology. It has been studied in many aspects by using various methods. Apomyoglobin is one of the proteins most extensively studied in the protein folding research.

It is known that apomyoglobin is stable in its native state at neutral pH and 30°C. The conformation changes cooperatively from native state to random coil between pH = 5 and 3.5 as shown by scanning microcalorimetry, viscosimetry, nuclear magnetic resonance, and circular dichroism spectrometry, electrometric, and calorimetric titration (Griko et al., 1988; Griko and Privalov, 1994). Three states are shown in the phase diagram of native (N), acid-induced molten globule (A), and acid-induced unfolded (U_A) states (Goto and Fink, 1990). The radius of gyration (R_g) of each state was measured by small angle x-ray scattering method (Kataoka et al., 1995). The R_g of molten globule (MG) state is close to that of N state rather than U_A state. The changes of thermodynamic parameters (enthalpy change (ΔH), entropy change (ΔS) and heat capacity change (ΔC_p)) corresponding to the transitions from N to MG (molten globule state) or MG to U (unfolded state), were summarized in the previous report (Nishii et al., 1995; see Table 2). In this paper, we examined N, A, and U_A states, following the phase diagram (Goto and Fink, 1990).

Protein structure is strongly related to protein-solvent interactions and hydration state. Among various methods, such as calorimetry, infrared spectroscopy, osmotic pressure analysis, dielectric spectroscopy, and nuclear magnetic resonance techniques, we used dielectric spectroscopy to study the hydration states of N, A, and U_A of apomyoglobin.

Dielectric spectroscopy provides direct information of the dynamic behavior of molecular dipole orientation in solution. The dielectric spectra of protein aqueous solution have usually manifest at least three relaxation processes called β, δ, and γ (Grant et al., 1978; Takashima, 1989).

One of the authors developed a method to measure the number of hydrating water molecules of several globular proteins (Suzuki et al., 1996). Here we applied this method to analyze δ and γ dispersions for protein solutions. We could then discuss the relation between structure change and hydration of protein, together with other thermodynamic parameters. This leads us to further understanding of intermediate protein structures in the unfolding process.

MATERIALS AND METHODS

Materials

Horse apomyoglobin was prepared by using Hapner's method (Hapner et al., 1968). Five-hundred milligrams of holomyoglobin (purchased from Sigma, St. Louis, MO, 99%) was dissolved in 20 ml of distilled water (Milli-Q purification, Millipore, Bedford, MA). First, this myoglobin solution was adjusted to pH 1.5 with HCl. Second, an equal volume of 2-butanone was added and mixed thoroughly. The butanone-rich layer containing heme was discarded. This extraction procedure was repeated twice. Third, a slightly brown colored aqueous layer was dialyzed against water until the pH of the protein solution became 5.0.

Finally, the three solutions of apomyoglobin in N, A, and U_A states were prepared with HCl at pH 5.0, 4.0, and 3.0, respectively. The reference solutions corresponding to N, A, and U_A states were prepared with HCl into water as those pH values become equal to 5.0, 4.0, and 3.0, respectively.

General description of dielectric spectroscopy

A typical dielectric absorption spectrum of protein solution has three peaks called β, δ, and γ dispersions. The β dispersion corresponds to the orientational relaxation of whole-protein dipole in water in the range from 0.1 to 2 MHz depending on the protein size. The γ dispersion is caused by orientational relaxation of free water dipoles at 17 GHz at 20°C. In the intermediate frequency range from 0.1 to 6 GHz we observe relatively

small δ dispersion caused by orientational relaxation of water molecules in the hydration shell of hydrophobic atom groups or in the hydration shell of free ions such as potassium ions, sodium ions, and halogen ions or the orientational relaxation of small dipolar organic molecules such as amino acids or glucose. Decreasing dielectric constant with increasing frequency indicates the sequential loss of polarizable elements in the solution. If we look at a spectrum of protein solution above 1 GHz the effect of β dispersion is negligible. The effect of ions and other small organic molecules can be easily excluded by subtracting the spectrum of the reference solution from that of protein solution. Thus, the dielectric constant in the gigahertz range provides the information of the volume of hydrated protein in bulk water.

One can derive the information of mobility of restrained (or bound) water from the dielectric relaxation spectra. The relaxation frequency, which is the peak frequency of the dielectric absorption, corresponds to the inverse of rotational time constant of poralizable elements such as water. Water molecules in the hydration shell of protein or in the bulk form thermally fluctuating hydrogen bonds with neighboring water or atoms of protein. Water molecules rotate according to the applied electric field direction by changing their hydrogen bond structure in a picosecond time scale. Water molecules rather strongly bound on polar atoms of protein surface have a low relaxation frequency below 1 GHz (Pennock and Schwan, 1969), and water molecules weakly restrained by atoms such as hydrophobic atoms have relatively high relaxation frequency ~5 GHz (Suzuki et al., 1996). Then we can detect weakly restrained bound water as well as strongly restrained water separately by using microwave of subgigahertz to 20 GHz. In this section we explain the method of analysis of protein hydration from the dielectric spectra.

Measurement

The dielectric spectra was obtained with a microwave network analyzer, Hewlett Packard 8720C, and open-end flat-surface coaxial probe. To avoid the accumulation of micro bubbles, the probe was fixed upward in a glass cell controlled at $20.0 \pm 0.01°C$ by a Neslab thermobath. The cell, made of pyrex glass, was of a conical shape with the dimension of 17 mm in inner diameter and a total volume of 3.2 ml. The solution temperature was monitored with a platinum-resistor thermosensor by using the four-terminal method. The cell was then filled with a sample-degassed solution. Microwaves in the frequency range from 0.2 to 20 GHz were introduced into the cell through the probe. The calibration was done by a procedure involving open termination in air, short termination with mercury, and soaking in pure water at $20.0 \pm 0.01°C$. The reflected waves were sampled by a network analyzer and converted to complex dielectric constants using HP85070A software following the Nicolson-Ross method.

The resolution of dielectric spectroscopy has been markedly raised by the following approach. The temperature T_{mx} of the microwave mixer of the network analyzer is responsible to the stability of baseline of the analyzer. For example, T_{mx} varied between 53 and 60°C without forced air flow and resulted in a large drift up to 0.3 in dielectric constant. The wave form of the T_{mx} change was of a saw-tooth shape, which consists of slow increase and sudden decrease. With the forced air flow system, T_{mx} was reduced to 34°C and its change reduced to 1°C, and resulted in a drift as small as 0.04 of a smooth waveform. Combining the forced airflow system with alternating measurements of sample solution and reference solution, the resolution of dielectric constant was successfully improved to 0.02. For each sample, 15 dielectric spectra of 51 frequency points from 0.2 to 20 GHz were sequentially obtained every 10 s at $20.0 \pm 0.01°C$ and then averaged.

We measured the dielectric spectra of sample solutions of three or four different concentrations and reference solution alternately to reduce machine drift. Then the accurate difference spectra between sample and reference solutions were obtained.
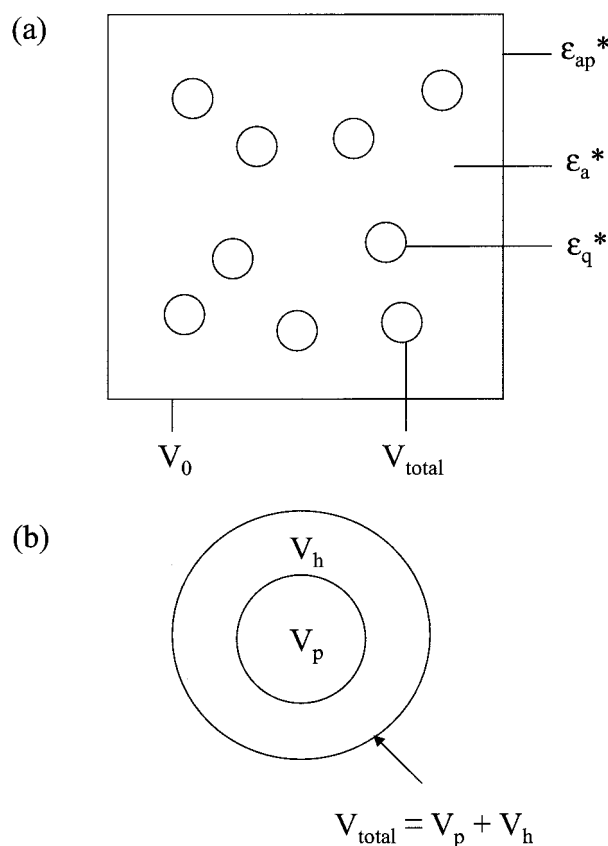

FIGURE 1 Schematic image of protein solution. (*a*) Protein solution. ϵ_{ap}^*, ϵ_a^*, and ϵ_q^* are the dielectric constants of protein solution, solvent, and solute, respectively. V_0 and V_{total} are the volumes of solution and a protein molecule with hydration shell, respectively. Definition of volume fraction φ: $\varphi = nV_{total}/V_0$. n is the total number of protein molecules in the solution. (*b*) Structure of hydrated solute. V_p and V_h are volumes of protein and hydrated shell, respectively. $V_{total} = V_p + V_h$, $\varphi_p = V_p/V_{total} = v/\varphi$, and $\varphi = nV_P/V_0$.

The density of protein solutions was measured with the density meter, Anton-Paar DMA-58 to obtain the partial specific volume, s_V of protein in solution.

The protein concentration was measured by the dry-weight method, whereby the protein solutions of 100 μl were dried in a vacuum chamber kept at 3 to 8×10^{-5} torr for 24 h at room temperature by a turbo molecular pump and a rotary pump. The dry weight of the protein was measured using an electronic balance (METTLER TOLEDO AG 285). If the value change between initial and final weights was more than 0.02 mg the sample was again placed in the vacuum chamber for another 5 h. This weight check was repeated until the value became stable.

Calculation of hydration number

We assumed that: 1) proteins in solution are spherical and have spherical hydration shells (Fig. 1); 2) solvents other than hydrated solutes have the same dielectric properties as those of pure solvents; 3) the dielectric constant of solute (protein) is constant, here we used 2.5 based on the electronic polarization of atom groups; 4) the dielectric constant of hydration shell at the high-frequency limit is 5.6, the same as that of pure water; and 5) total hydration shells have a dielectric relaxation of a single

Debye-type in the GHz range. This fifth assumption is for the simplest case, which has a single relaxation process.

The apparent complex dielectric constant ϵ_{ap}^* of the protein solution is expressed with the dielectric constant of solvent ϵ_a^* and that of dispersed solutes ϵ_q^* as

$$\varepsilon_{ap}^* = \varepsilon_a^* \frac{2(1-\varphi)\varepsilon_a^* + (1+2\varphi)\varepsilon_q^*}{(2+\varphi)\varepsilon_a^* + (1-\varphi)\varepsilon_q^*}$$

(Wagner equation (Wagner, 1914) for $\varphi \ll 1$)

(1)

in which φ is the volume fraction of the hydrated solute; $\varphi = n V_{total}/V_0$ as shown in Fig. 1 a. n is the total number of solutes. When the solute is a spherical protein with a hydration shell, ϵ_q^* is again expressed with the dielectric constant of the hydration shell ϵ_h^* and that of the core (protein) ϵ_p^* by Wagner equation.

$$\varepsilon_q^* = \varepsilon_h^* \frac{2(1-\varphi_p)\varepsilon_h^* + (1+2\varphi_p)\varepsilon_p^*}{(2+\varphi_p)\varepsilon_h^* + (1-\varphi_p)\varepsilon_p^*}$$

(for $0 < \varphi_p < 1$), (2)

in which $\varphi_p = v/\varphi = V_p/V_{total}$ as shown in Fig. 1 b. v is the volume fraction of protein in solution calculated by $cM_ws_v/1000$. c, M_w, and s_v are the concentrations of protein in moles/liter, molecular weight in grams, and the partial specific volume of protein in liters/kilograms, respectively. $s_V = \lim (1 - \Gamma)/c'$ $(c' \rightarrow 0)$, $\Gamma = (d - c')/d_0$, in which d is the density of the protein solution; d_0, the density of the reference solution; $c' = cM_w/1000$, the concentration of solute in kilograms per liter; $\Gamma = 1 - v$, the apparent volume fraction of solvent in solution. We adopted the s_V values: 0.76 (l/kg) for N; 0.75 for A; and 0.74 for U_A state. Eq 2 is used to obtain $\epsilon_{q\infty}$, the high frequency limit $(f \rightarrow \infty)$ of ϵ_q^*, in which $\epsilon_h^* = \epsilon_{h\infty} = 5.6$ and $\epsilon_p^* = \epsilon_{p\infty} = 2.5$ were used for $f \rightarrow \infty$ by the third and fourth assumptions.

The procedure to obtain ϵ_q^* is as follows. First, assuming a small initial value of φ, the dielectric spectrum of the hydrated solute ϵ_q^* was calculated by Eq. 1 using measured ϵ_{ap}^* and ϵ_a^*. Second, the obtained ϵ_q^* was fitted with a single Debye relaxation function in the high frequency range of 5.0 to 17.0 GHz,

$$\varepsilon_q^* \approx \varepsilon_{q\infty} + \frac{(\varepsilon_{qs} - \varepsilon_{q\infty})}{1 + j(f/f_c)}$$

(3)

Here, the value $\epsilon_{q\infty}$ may become negative for very small φ. However the actual value of $\epsilon_{q\infty}$ must be positive and close to the value given by Eq. 2 at $f \rightarrow \infty$. Third, φ was iteratively adjusted in Eqs. 1 and 2 until $\epsilon_{q\infty}$ in Eq. 3 agreed with the value obtained by Eq. 2. Thus, we obtained φ, f_c, ϵ_{qs}, and $\epsilon_{q\infty}$.

This fitting range was chosen for the following reasons: Eq. 3 is only valid for a single relaxation process, which may occur at the high frequency range close to 17 GHz. The low frequency limit was chosen as 5 GHz, which was reported previously as the relaxation frequency of the hydrophobic hydration shell (Suzuki et al., 1997a).

The total number of restrained water molecules per protein molecule N_{total} was then calculated as follows

$$N_{total} = \frac{55.6(\varphi - v)\rho_{hyd}}{c}$$

(4)

in which ρ_{hyd} is the density of the hydration shell, which was set at 1.0 kg/l according to the definition of partial specific volume. Because v is the virtual volume fraction of proteins measured from the solution density with a two-component model consisting of pure solute and pure solvent.
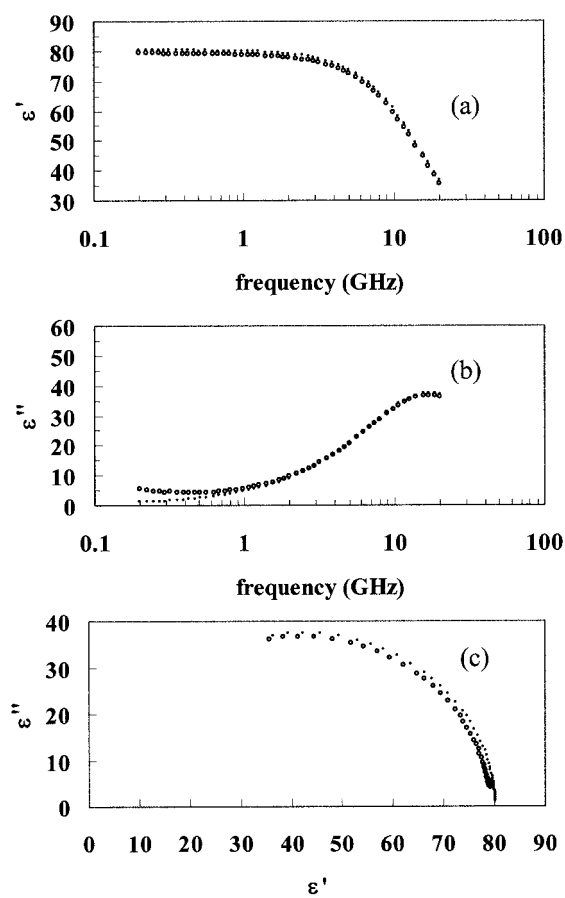
FIGURE 2 Microwave dielectric spectra of apomyoglobin solution and water. Circles indicate apomyoglobin solution (N state at 14.6 mg/ml); dots indicate reference solution (water). (a) Real part of dielectric constant; (b) imaginary part of dielectric constant; (c) Cole-Cole plots of dielectric constant

RESULTS

Dielectric spectra of apomyoglobin solutions

Fig. 2 (a and b) shows the dielectric spectrum of apomyoglobin solution and water. The complex dielectric constant of solution ϵ^* is divided into the real part ϵ' (Fig. 2 a) and the imaginary part ϵ'' (Fig. 2 b), $\epsilon^* = \epsilon' - j\epsilon''$. Fig. 2 c is the Cole-Cole plots of the apomyoglobin solution (circles) (N state at 14.6 mg/ml as an example) and reference solution (dots), which is a hydrochloric acid solution of pH = 5 and actually equivalent to pure water in ϵ'. Because the difference between the protein solution and reference solution is so small we show the difference spectra ($\Delta\epsilon'$ and $\Delta\epsilon''$) derived by calculating the protein solution dielectric constant ϵ_{ap}^* minus the reference solution dielectric constant ϵ_a^*, $\Delta\epsilon^* = \epsilon_{ap}^* - \epsilon_a^*$ in Fig. 3.

Fig. 3 shows the difference dielectric spectra $\Delta\epsilon'$ of apomyoglobin (N, A, and U_A states) solutions, respectively. The minimal value of $\Delta\epsilon'$ around 7 GHz for each curve is proportional to the total volume of hydrated solute. More
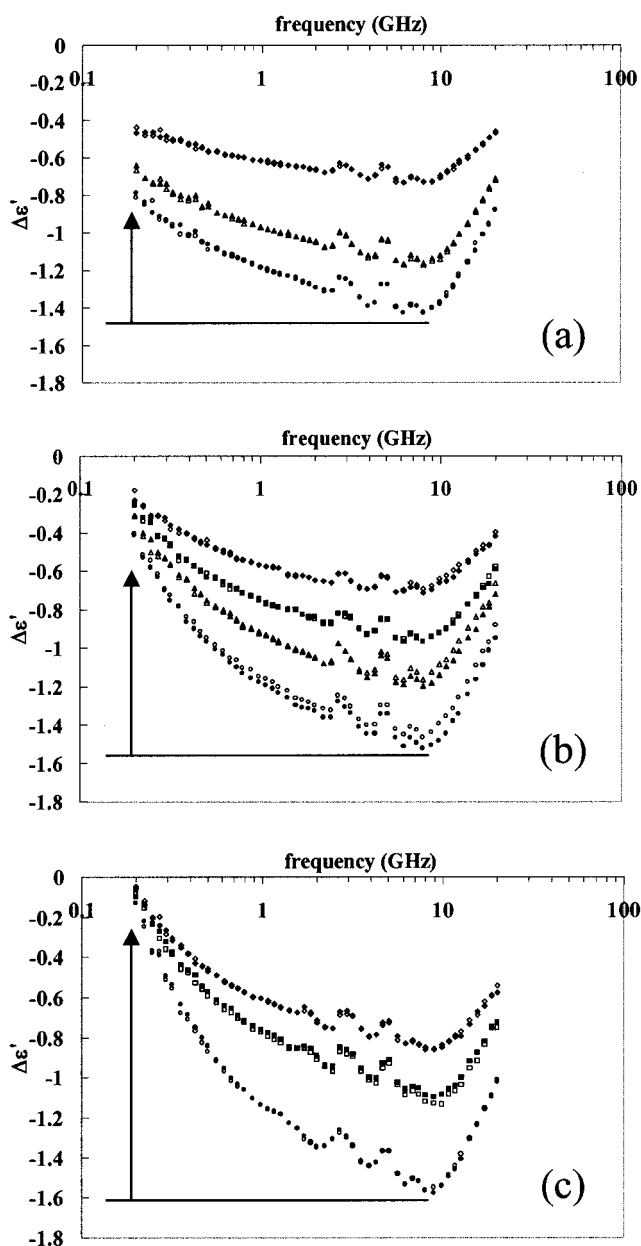
FIGURE 3 Real part of dielectric constant $\Delta\epsilon'$ versus frequency for N, A, and U_A states. The dielectric spectra were measured twice at each concentration: the first measurements are shown with open symbols and the second with filled symbols. (*a*) N state of apomyoglobin; the concentrations were 7.3, 12.1, and 14.6 mg/ml from the top, respectively. (*b*) A state of apomyoglobin; the concentrations were: 7.3, 9.7, 11.9, and 14.0 mg/ml from the top, respectively. (*c*) U_A state of apomyoglobin; the concentrations were 6.5, 8.8, and 12.8 mg/ml from the top, respectively.
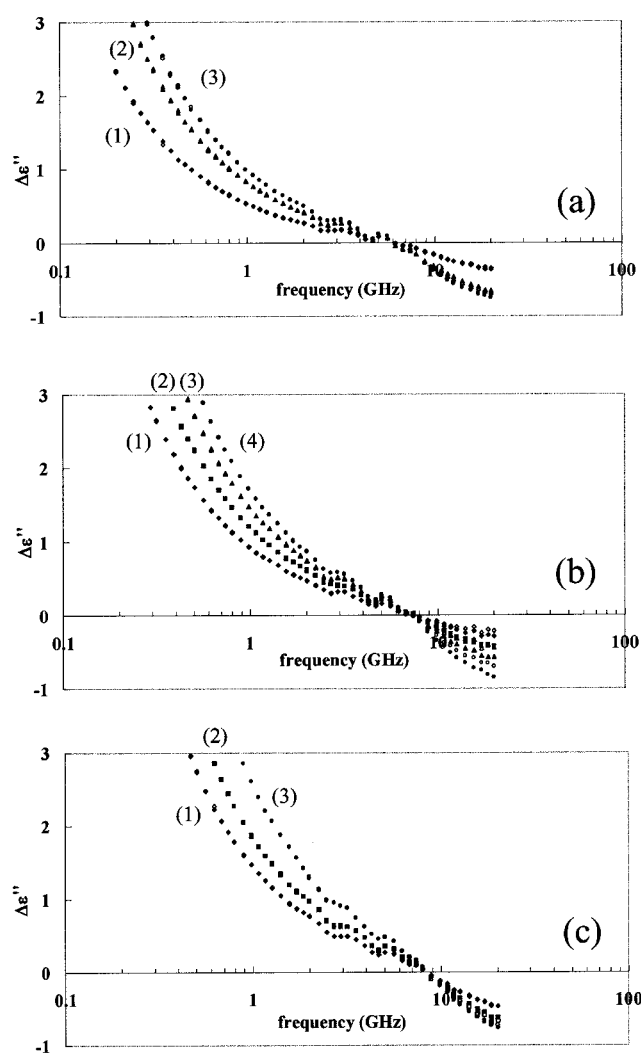

FIGURE 4 Imaginary part of dielectric constant $\Delta\epsilon''$ versus frequency corresponding to Fig. 3. The dielectric spectra were measured twice at each concentration: the first measurements are shown with open symbols, the second with filled symbols. (*a*) N state of apomyoglobin; the concentrations of each spectrum were: (*1*) 7.3, (*2*) 12.1, and (*3*) 14.6 mg/ml. (*b*) A state of apomyoglobin; the concentrations of each spectrum were: (*1*) 7.3, (*2*) 9.7, (*3*) 11.9, and (*4*) 14.0 mg/ml. (*c*) U_A state of apomyoglobin; the concentrations of each spectrum were: (*1*) 6.5, (*2*) 8.8, and (*3*) 12.8 mg/ml, respectively.

U_A (triangles) states. This indicates that protein molecules in N, A, and U_A states are monodispersed, then we may neglect interactions among protein molecules such as dimerization or aggregation.

In the subgigahertz range (Fig. 3), we observed another polarization indicated by arrows that increased for the transitions from N to A and from A to U_A.

Hydration numbers of apomyoglobin at N, A, and U_A states

Fig. 6 shows single Debye fitting by Eqs. 1 and 3 for the spectra on Fig. 3 (N state at 14.6 mg/ml; A state at 14.0 mg/ml; or U_A state at 12.8 mg/ml for example) and the

detailed explanations are given in the Appendix 1. The curves of $\Delta\epsilon''$ are shown in Fig. 4. In this study $\Delta\epsilon''$ curves were not used for quantitative analysis but only used for the examination of Eq. 3.

Fig. 5 shows linear relations between protein concentration and $\Delta\epsilon'$ at 8.9 GHz for N (circles), A (rectangles), and
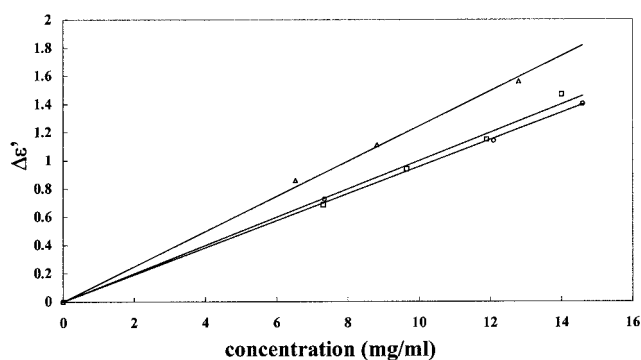
FIGURE 5 Relationship between concentration and $\Delta\epsilon'$; N state of apomyoglobin ($\bigcirc$); A state of apomyoglobin ($\square$); U$_A$ state of apomyoglobin ($\triangle$).

hydration numbers, N_{total}, were calculated based on the Wagner equation (Wagner, 1914), Eq. 1, and Eq. 4. The method of calculation of hydration numbers was explained in detail in Materials and Methods section. Table 1 shows the hydration numbers of apomyoglobin as: 590 for N state; 630 for A state; and 1110 for U$_A$ state.

Error analysis

The absolute error of the measured value N_{total} should originate from impurities, the stability of the network analyzer, the error of the protein concentration, the error of partial specific volume of protein molecules, and $\epsilon_{q\infty}$, the shape of protein, and/or the plausibility of Debye relaxation for restrained water.

Impurities

The purity of the purchased holomyogobin was 99% according to Sigma's data. Acid-induced hydrolysis of protein

TABLE 1 Properties of hydration shells for N, A, and U$_A$ states

State	Concentration (mg/ml)	f_c (GHz)	$\varepsilon_{qs} - \varepsilon_{q\infty}$	N_{total}
N		6.9	26	617
M_W 17,000 s_V 0.76	7.34	6.8	25	584
	12.1	6.8	27	587
		6.8	26	562
	14.6	6.8	26	582
		6.9	27	608
	Average			590
	SD			18
A		6.3	22	448
M_W 17,000 s_V 0.75	7.31	6.4	25	528
	9.65	6.7	28	636
		6.7	29	660
	11.9	6.4	24	516
		6.5	28	629
	14.0	6.7	27	669
		6.8	29	805
	Average			630
	SD			104
U$_A$		7.1	29	1246
M_W 17,000 s_V 0.74	6.53	7.1	29	1168
	8.82	7.1	29	1160
		7.1	29	1068
	12.8	7.1	29	1081
		7.1	29	1049
	Average			1110
	SD			65

f_c, relaxation frequency; $\varepsilon_{qs} - \varepsilon_{q\infty}$ are given by Eq. 3.

is thought to be negligible during the dielectric measurement for several hours after the addition of a small amount of acid. The residual holomyoglobin fraction (containing heme) in the tested apomyoglobin solutions was estimated from the absorbance at 408 and 280 nm. The contamination ratio of holomyoglobin was calculated to be 1% in all three
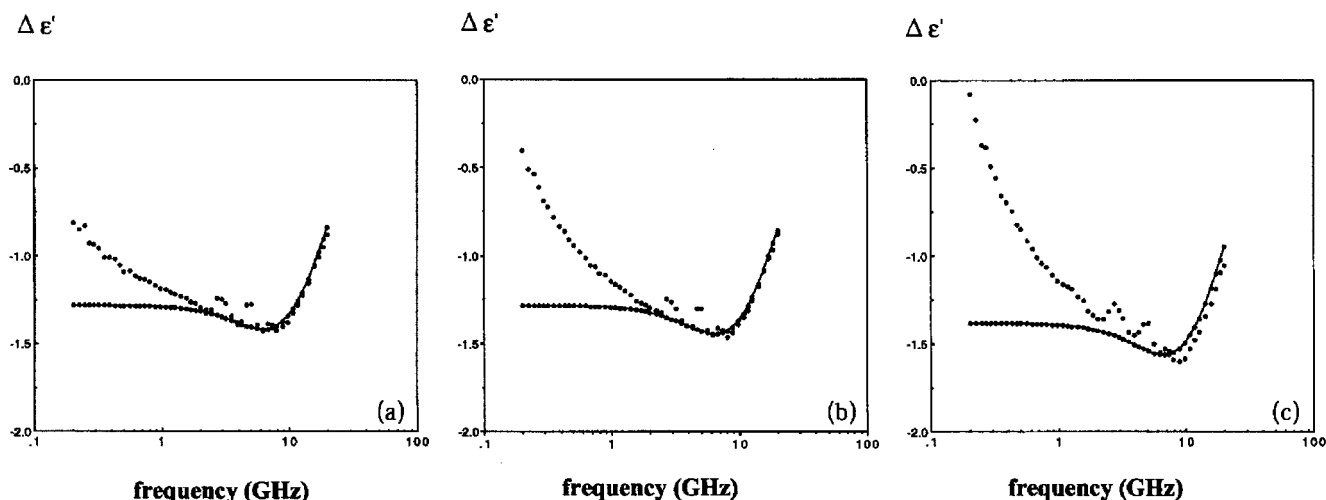

FIGURE 6 $\Delta\epsilon'$ spectra with single Debye fitting by Eqs. 1 and 3. (a) N state of apomyoglobin, 14.6 mg/ml. (b) A state of apomyoglobin, 14.0 mg/ml. (c) U$_A$ state of apomyoglobin, 12.8 mg/ml.

states. Therefore, the error of the hydration number from impurites is negligible.

Machine noise

As noted in the Method section, the resolution of dielectric constant at each frequency was 0.02. Therefore, the standard deviation of hydration number was estimated as being 63 for apomyoglobin solution over 20 measurements.

Concentration

By the process of determining the weight of apomyoglobin, there might be ± 0.01 mg error. The error of N_{total} was at most ± 10 in N state, ± 30 in A state, and ± 20 in U_A state.

Partial specific volume

The values of partial specific volume were obtained as mean values, considering the deviations of s_v's: 0.006 for N; 0.017 for A; and 0.007 for U_A. The error of N_{total} was at most ± 10 in N state, ± 20 in A state, and ± 10 in U_A state.

Influence of HCl

We also have to consider the volume fraction of ions. In this experiment, this effect was insignificant. The maximal effect of HCl on ϵ' was found at 3 GHz. At 100 mM HCl solution, the $\Delta\epsilon'$ was -0.35 at 3 GHz, so in the case of 1 mM (pH 3), the $\Delta\epsilon'$ is -0.0035. Because we analyzed the difference between the protein solution and the reference solution, the error caused by HCl is negligible.

Shape of protein

As a protein molecule changes from N to A or from A to U_A, the shape of protein varies from globule to coil. We examined the shape-effect on the estimated hydration numbers using oligo-saccharide solutions as noted in Appendix 2. As a result, we conclude the estimation is not sensitive to the molecular shape.

Considering all of the factors above mentioned, N_{total} with the errors were presented in Table 2.

DISCUSSIONS

Table 3 is a summary of physical parameters according to Nishii et al. (1995). The ratios of helical content were 55% in N state, 30% in A state, and 5% in U_A state. Although the change of helical content from N to A is similar to that from A to U_A, the behavior of the hydration numbers in our experiment was different. The hydration numbers of N and A states were very close to each other. This result indicates that A state has a compact structure like N state despite the disruption of the helical structure and that hydrophobic

TABLE 2   Errors of hydration numbers for N, A, and U_A states

State	N	A	U_A
N_{total} (from Table 1)	590 (SD 18)	630 (SD 104)	1110 (SD 65)
	The hydration number error		
Error factor			
Machine noise	± 63	± 63	± 63
Concentration	± 10	± 30	± 20
s_V	± 10	± 20	± 10
N_{total} with error	590 ± 65	630 ± 73	1110 ± 67

moieties of A state were not exposed to solvent as imaged in Fig. 7. The previous work (Suzuki et al., 1997a,b) demonstrated that hydrophobic moieties at the protein surface are responsible for the total hydration of proteins. As shown in Table 3, a large decrease of ΔC_p from N to MG suggests association of hydrophobic moieties at the protein surface. If association of hydrophobic moieties occurs at the protein surface, considerable dehydration will be observed. On the other hand, the decrease of helical content from N to A should lead fairly large exposure of the peptide chain. As a total, these two effects on the total hydration may cancel each other.

The x-ray scattering study of gyration radius (Kataoka et al., 1995; Table 3) supports this structural compactness of A state. On the other hand, the hydration number of U_A state was large compared with that of A state. In the U_A state, a part of the broken helical structure may be exposed to solvent, or a frame-forming tertiary structure may be extended.

It is note worthy that U_A was more compact than expected. Theoretically, the predicted hydration number of linearly extended structure is 1340, ~200 larger than the experimental value. The theoretical hydration number of a linearly extended structure was calculated from the accessible surface area of each amino acid residue (Suzuki et al., 1997b). The experimental number might include second

TABLE 3   Comparison of the structure and thermodynamic properties of apomyoglobin summarized by Nishii et al. (1995)

State	Rg (Å)	$\Delta C_{p,u}$ (kJ mol^{-1} K^{-1})	Helical content (%)
Holomyoglobin			
N	17.5	8.7*	66
Apomyoglobin			
N	20.1	4.0*	55
MG	22.2	2.3[†] (1.8*)	45
		1.7[†] (3.1[‡], 1.5*)	28
A			30[§]
U_A	29.3	0	5

*Values taken from Nishii et al. (1994).
[†]Values obtained from the unfolding curves measured by CD.
[‡]Value obtained from the DSC curves.
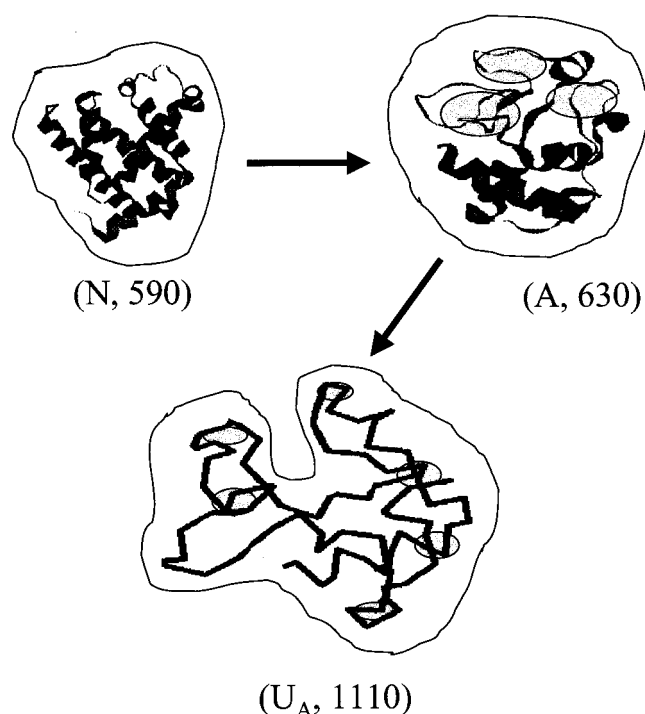[§]Value calculated from the phase diagram.

FIGURE 7 Conceptual image of three states, N, A, and U$_A$ of apomyoglobin. In the parentheses, the total hydration numbers are shown. The shaded parts indicate the region of hydrophobic association. The contours show the total volume of hydrated protein.

layer, if any. Therefore, because the experimental estimation was smaller than the theoretical number, the U$_A$ state should not be a fully exposed random coil as in Fig. 7.

APPENDICES

Appendix 1: How to derive information from Fig. 3

First, let us consider small air bubbles homogeneously mixed in water. The volume fraction of bubbles is $\varphi = 0.01$. Wagner Eq. 1 gives the total dielectric constant of the mixture ϵ_{ap}. The difference dielectric constant $\Delta\epsilon$ of the mixture is obtained by subtracting the dielectric constant ϵ_w of water from that of the mixture. In Fig. 8 the open rectangles are for $\Delta\epsilon'$ (real) and open circles for $\Delta\epsilon''$ (imaginary). Below 3 GHz $\Delta\epsilon'$ is constant, and above 3 GHz it approaches asymptotically to the baseline (water, or the reference solution level). This increase at high frequency is due to the dielectric relaxation property of bulk water or reference solutions. When a solute instead of a bubble has a relaxation frequency, f_c, of 5 GHz $\Delta\epsilon'$ and $\Delta\epsilon''$ are shown as filled diamond (real) and filled triangles (imaginary). The broken line, which equals to (filled diamonds minus open rectangles) and the solid line (filled triangles minus open circles) show the dielectric relaxation property of the solute. Therefore the increase of $\Delta\epsilon'$ above 10 GHz is due to the bulk water. The depth of the $\Delta\epsilon'$ ~7 GHz is proportional to the amount of the hydrated solutes. In the experiment in Fig. 3, one finds gradual increase toward low frequency, which mechanism is unclear but possibly due to the mobile polar chains induced by unfolding of protein molecule.
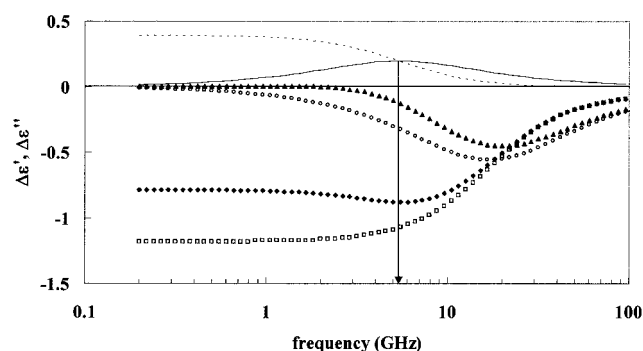
FIGURE 8 Calculated difference spectra of dielectric constant $\Delta\epsilon'$ and $\Delta\epsilon''$. The difference dielectric spectra with $f_c = 5$ GHz in Eq. 3. $\Delta\epsilon'$ ($\square$) and $\Delta\epsilon''$ ($\bigcirc$) are the real and imaginary parts of difference dielectric constant, respectively, calculated for air bubbles in water with volume fraction $\varphi = 0.01$ based on Eq. 1 (see Materials and Methods). $\Delta\epsilon'$ ($\blacklozenge$) and $\Delta\epsilon''$ ($\blacktriangle$); values calculated for solutes with $f_c = 1$ GHz at $\varphi = 0.01$ based on the equation $\epsilon_q^* = 1.0 + 20/\{1 + j(f/f_c)\}$ and Eq. 1. (*Solid line*) Difference between triangles and circles; (*broken line*) difference between diamonds and squares.

TABLE 4 Estimation of hydration numbers for linear sugars by Eqs. 1 through 4

Degree of polymerization	ASA (Å)	N_{total}
1	322	12
2	487	24
3	646	34
5	965	54

1, D-Glucose; 2, maltose; 3, maltotriose; 5, maltopentase.
ASA, accessible surface area was calculated on the surface formed by the center of each water molecule with a radius of 1.4 Å in the first hydration shell accessible to solute molecule.

Appendix 2

We applied Wagner Eq. 1 assuming a spherical model to analyze A and U$_A$ states as well as N state for the following reasons: based on Wagner Eq. 1, we measured the dielectric constants of several oligo-saccharides, D-glucose as a model of a sphere, maltose as a dimer, maltotriose as a trimer, and maltopentaose as a pentamer. The results are shown in Table 4. The increment of N_{total} per monomer unit was found to be 10, which was insensitive to the polymerization degree. This simple model experiment supports the application of the Wagner equation to A or U$_A$ states. Further quantitative examination remains for future studies.

REFERENCES

Goto, Y., and A. L. Fink. 1990. Phase diagram for acidic conformational states of apomyoglobin. *J. Mol. Biol.* 214:803–805.

Grant, E. H., R. J. Sheppard, and G. P. South. 1978. Dielectric Behavior of Biological Molecules in Solution. Clarendon Press, Oxford.

Griko, Y. V., and P. L. Privalov. 1994. Thermodynamic puzzle of apomyoglobin unfolding. *J. Mol. Biol.* 235:1318–1325.

Griko, Y. V., P. L. Privalov, S. Y. Venyaminov, and V. P. Kutyshenko. 1988. Thermodynamic study of the apomyoglobin structure. *J. Mol. Biol.* 202:127–138.

Hapner, K. D., R. A. Bradshaw, C. R. Hartzell, and F. R. N. Guard. 1968. Comparison of myoglobins from harbor seal, porpoise, and sperm whale. *J. Biol. Chem.* 243:683–689.

Kataoka, M., I. Nishii, T. Fujisawa, T. Ueki, F. Tokunaga, and Y. Goto. 1995. Structural characterization of the molten globule and native states of apomyoglobin by solution x-ray scattering. *J. Mol. Biol.* 249:215–228.

Nishii, I., M. Kataoka, and Y. Goto. 1995. Thermodynamic stability of the molten globule states of apomyoglobin. *J. Mol. Biol.* 250:223–238.

Nishii, I., M. Kataoka, F. Tokunaga, and Y. Goto. 1994. Cold denaturation of the molten globule states of apomyoglobin and a profile for protein folding. *Biochemistry.* 33:4903–4909.

Pennock, B. E., and H. P. Schwan. 1969. Further observations on the electrical properties of hemoglobin-bound water. *J. Phys. Chem.* 73:2600–2610.

Suzuki, M., J. Shigematsu, Y. Fukunishi, Y. Harada, T. Yanagida, and T. Kodama. 1997b. Coupling of protein surface hydrophobicity change to ATP hydrolysis by myosin motor domain. *Biophys. J.* 72:18–23.

Suzuki, M., J. Shigematsu, Y. Fukunishi, and T. Kodama. 1997a. Hydrophobic hydration analysis on amino acid solution by the microwave dielectric method. *J. Phys. Chem.* 101:3839–3845.

Suzuki, M., J. Shigematsu, and T. Kodama. 1996. Hydration study of proteins in solution by microwave dielectric analysis. *J. Phys. Chem.* 100:7279–7282.

Takashima, S. 1989. Electrical Properties of Biopolymers and Membrane. Adam Hilger, Bristoland, Philadelphia, PA.

Wagner, K. W. 1914. Erklärung der dielektrischen Nachwirkungsvorgänge auf Grund Maxwellscher Vorstellungen. *Archiv. Elektrotechink.* 2:371–387.